

**NASA TECHNICAL  
MEMORANDUM**

NASA TM X-52452

NASA TM X-52452

FACILITY FORM 602

N 68-31043 (ACCESSION NUMBER)	(THRU)
15 (PAGES)	(CODE)
✓ (NASA CR OR TMX OR AD NUMBER)	(CATEGORY)

**THE DOUBLE CONTAINMENT TANTALUM-STAINLESS  
STEEL SNAP-8 BOILER**

by L. W. Gertsma, P. A. Thollot, D. W. Medwid,  
and A. J. Sellers  
Lewis Research Center

TECHNICAL PAPER proposed for presentation at  
Intersociety Energy Conversion Engineering Conference  
Boulder, Colorado, August 13-16, 1968



NATIONAL AERONAUTICS AND SPACE ADMINISTRATION · WASHINGTON, D.C. · 1968

**THE DOUBLE CONTAINMENT TANTALUM-STAINLESS**

**STEEL SNAP-8 BOILER**

by L. W. Gertsma, P. A. Thollot, D. W. Medwid, and A. J. Sellers

Lewis Research Center  
Cleveland, Ohio

**TECHNICAL PAPER** proposed for presentation at  
Intersociety Energy Conversion Engineering Conference  
Boulder, Colorado, August 13-16, 1968

**NATIONAL AERONAUTICS AND SPACE ADMINISTRATION**

# THE DOUBLE CONTAINMENT TANTALUM-STAINLESS STEEL

## SNAP-8 BOILER

by L. W. Gertsma, P. A. Thollot, and D. W. Medwid  
Lewis Research Center  
National Aeronautics and Space Administration  
Cleveland, Ohio

and A. J. Sellers  
Aerojet-General Corporation  
Azusa, California

### ABSTRACT

One of the major problem areas in the development of the SNAP-8 space power system has been the mercury boiler, principally due to the incompatibility of containment materials with mercury. As an approach to the solution to this basic problem, a boiler utilizing tantalum for the mercury-containment material was designed for the SNAP-8 system and tested at the NASA-Lewis Research Center for 1445 hours. Because of safety requirements, the design incorporated double containment of the mercury, which in effect separated the radioactive primary loop fluid from the mercury by two metal walls and a buffer region filled with NaK. Design features which enabled the use of a tantalum tube within a stainless steel (SS) tube are discussed. These include both an oval SS containment tube and a bellows to allow for differential thermal expansion and the need for bimetallic joints. Thermal design of the boiler is described. The overall operating history and a comparison of test results with predicted performance indicate the boiler fulfilled its design requirements.

### INTRODUCTION

In a Rankine cycle space power system such as SNAP-8<sup>(1)</sup>, a key requirement is the dependable generation of dry, superheated vapor immediately upon startup. Using mercury as the two-phase power fluid has presented problems in the past. The most serious problem has been the incompatibility of most alloyed containment materials with mercury in two-phase forced-convection flow conditions. Furthermore, boiler performance has been shown to depend to a large degree on whether or not mercury was wetting the heat transfer surfaces<sup>(2)</sup>. Previous work<sup>(2,3)</sup> has indicated that the degree of wetting, sometimes referred to as boiler conditioning, is largely dependent on the mercury-containment material, tube surface oxides, and trace amounts of impurities such as hydrocarbons. Test results have shown that boiler performance improves with time due to the scrubbing action of high-velocity mercury, and that wetting agents such as

rubidium improve boiler performance. However, in order to satisfactorily fulfill system requirements, boiler performance should not be time dependent or rely on wetting agents. A new design concept was developed, utilizing tantalum's desirable properties such as low solubility, corrosion resistance, and good wettability as the mercury-containment material. In order to meet the specifications for a man-rated system which require double isolation between the radioactive primary-loop fluid and the power-loop mercury, a buffer or static-fluid region was incorporated in the boiler design. The use of tantalum (Ta) together with stainless steel (SS) required new techniques in mechanical design and fabrication. The SS is necessary for primary NaK containment because of oxygen contamination of the Ta. The design configuration, thermal analyses, fabrication, and the results of 1445 hours of testing are discussed herein.

### DESCRIPTION

A pictorial representation of the double-containment Ta-SS boiler showing areas of principal interest is given in Fig. 1. Tantalum was selected for the mercury-side containment material based on its very low solubility in liquid mercury (see Fig. 2) and its apparently good wettability by mercury at SNAP-8 temperatures. The cross-sectional view shown in Fig. 1(a) illustrates the manner in which the double-containment of the mercury was achieved. In effect the radioactive primary loop NaK is separated from the mercury loop by two metal walls and a static NaK region. NaK-78, the eutectic mixture of sodium and potassium, was used in this buffer region because of its excellent heat-transfer characteristics. Flow conditions in the boiler are NaK flowing counter to mercury. Mercury flows through a tantalum tube which is surrounded by stagnant NaK contained in an oval-shaped SS tube. Seven such Ta-SS tube assemblies placed in parallel form a bundle 34 ft (11300 mm) long (see Fig. 3). The tube bundle which is coiled to a mean helix diameter of 48 inches (1220 mm) is in turn surrounded by an outer shell within which the primary-loop NaK flows. A 4.5-ft-long (1370 mm) multipassage plug insert is used to increase local velocities in the preheat and low-vapor-quality region of the boiler (see Fig. 1(b)). A swirl-wire turbulator is used in the remainder of the open tantalum

tube. A fixed orifice placed at the entrance of each of the seven tantalum tubes provides mercury-flow stabilization<sup>(4)</sup>. Shown in Fig. 4 are the pieces which comprise the plug section. Illustrated in Fig. 1(c) are details of the mercury-exit configuration.

#### DESIGN CONFIGURATION AND FABRICATION

A number of problems were encountered in the design and fabrication of this boiler because of the use of tantalum and stainless steel in its construction. The most serious problem encountered resulted from the fact that the coefficients of thermal expansion for stainless steel and tantalum differ. This difference is approximately  $7 \times 10^{-6}$  in/in/ $^{\circ}$ F between room temperature and  $1300^{\circ}$  F ( $978^{\circ}$  K). As a result, the growth difference of a concentric tube-in-tube assembly (see Fig. 3) between these temperatures would be about 4 in. (100 mm). To avoid taking a growth difference of this magnitude at the end of the tubes, the design allowed for radial movement of the tantalum tube within the flattened stainless tube. In effect the location of the tantalum tube within the stainless steel tube moves from one side to the other; see Fig. 1(a). By flattening the 1.00 in. (25.4 mm) diameter stainless steel tube to 0.78 in. (19.8 mm) between the flat, 0.28 in. (7.1 mm) movement was available. It is estimated that 0.2 in. (5.1 mm) would be required to take up the total thermal expansion difference.

In order to cut lead times in the procurement of materials, standard tube sizes were used wherever possible. Previous work (Ref. 5) provided general background information used in the design of this boiler. The resultant configuration consisted of a tantalum tube 0.75 in. (19.0 mm) outside diameter (O.D.), with a 0.040 in. (1.0 mm) wall thickness, and a stainless steel (type 321) tube 1.00 in. (25.4 mm) O.D. with a 0.035 in. (0.89 mm) wall which was flattened as described earlier. A bundle of seven such tube-in-tube assemblies were symmetrically arranged within a single 5.0 in. (127 mm) O.D.  $\times$  0.095 in. (2.40 mm) wall stainless steel (type 316) tube.

Tantalum, although highly resistant to mercury corrosion, is very susceptible to oxidation at elevated temperatures. This, of course, presented a problem not only during system operation but in fabrication as well since all welding involving tantalum had to be done either in a vacuum chamber or in an inert atmosphere. Consequently, a vacuum chamber with a rotating-head electron-beam machine was used to weld the tantalum tubing to the desired length (see Fig. 5). Tube-to-header welds were difficult because of the concentric-tube configuration. To facilitate the stainless header welds and to reduce the stress at the end of the tubes, short heavy-wall sections were added to the stainless tubes before assembly. These heavy sections were then welded into the stainless header with a full-penetration weld, after which a heavy filler pass was made. The tantalum tubes were expanded into grooves in the tantalum header and a fusion lip-seal weld was used (see Fig. 6).

A bimetal joint of tantalum to stainless steel was needed at both ends of the boiler for attachment of the floating tantalum tubes to the stainless steel shell. This joint is a tongue-in-groove connection brazed with J-8400 alloy. Tests of this joint are reported in Ref. 6.

To complete the attachment to the shell, a stainless steel (type 321) three-ply bellows was used at both ends of the boiler. The transition dome, bimetal joint, and bellows formed a separate subassembly (see Fig. 7). In welding the transition dome (see Fig. 7) to the tantalum header plate shown in Fig. 6, a portable glove box purged with argon was used. At the time of assembly, convoluted 5-mil-thick zirconium foil was wrapped around this subassembly to act as a getter for any oxygen possibly present in the static NaK. The outer shell was separately coiled and cut into short lengths of approximately 4 ft (1220 mm). Each section was slipped over the tube bundle and welded.

A unique technique was developed for coiling the long tantalum-within-stainless tube sections. It was important that the tantalum tube touch the outer wall of the stainless oval when cold (see Fig. 1(a)) so that when hot the differential expansion could be taken up by radial movement. Therefore, to assure proper tube location during coiling, a flexible hose was placed in the open area between the two tubes and filled with water. Cold alcohol was then circulated through the tantalum tube to freeze the water in the flexible hose which maintained the relative tube positions during the coiling operation. A finger pump was used to continuously circulate the alcohol throughout the coiling operation, and dry ice provided the cooling. Cleaning the coiled sections was simply a matter of heating and flushing with a mild solvent.

#### THERMAL DESIGN

The design approach was based on SNAP-8 boiler development test results and analytical correlations. Forced-convection dropwise dry-wall mercury boiler theory<sup>(7,8)</sup> was utilized to establish the mercury heat and momentum transfer parameters. To enable one-dimensional nodal heat and momentum transfer analysis, the actual double-containment oval-and-round tube geometry was simplified to a concentric tube-in-tube configuration. The NaK flow passage was sized based on available conductances and prescribed pressure drop limitations. Results of the NaK side heat and momentum transfer analysis are presented in Fig. 8. Shown are values of the NaK side pressure drop ( $\Delta P_N$ ) and film coefficient ( $h_N$ ) in terms of the oval tube spacing (S).

A multipassage-plug insert and swirl-wire turbulator were used to establish vortex flow in the boiling region. This design serves the added function of creating centrifugal forces which tend to make the boiler's operation insensitive to the gravity environment. Past experience has shown that dropwise dry-wall boiling theory<sup>(7)</sup> predicts conservative boiler performance for conditioned

mercury-flow passage surfaces. For the case where surface wetting in the low-vapor-quality region exists, boiler performance may be better than predicted by this design approach, resulting in greater superheat.

The basic method of analysis was to subdivide the boiler length into a series of small increments and to write the coupling heat-transfer and pressure drop correlations for each increment. The boiler preheat and superheat sections were subdivided by taking equal increments of the mercury temperature rise. Similarly, the wet-vapor region was subdivided by taking equal increments of vapor quality. The solution of the coupling equations at each node provided the local thermal and dynamic operating parameters, increment length, and node-boundary state conditions. Sequential solution of the nodal equations using standard computer techniques resulted in the determination of the overall boiler performance. Presented in Refs. 7, 8, 9, 10, and 11 are the momentum-transfer correlation equations used for non-wetting boiling, intermittent-contact boiling, and film boiling. The type of boiling process and the two-phase pressure drop correlations used in the analysis are also discussed in these references.

The predicted boiler performance characteristics at nominal operating conditions are shown in Fig. 9. The nominal boiler NaK-inlet temperature of 1305° F (980.4° K) was used for this plot. Figure 9 shows that the maximum heat flux ( $q''$ ) occurs in the preheat section. Within the preheat section,  $q''$  is a minimum at the liquid-vapor interface and asymptotically approaches the ordinate at zero preheat length. A plot of the heat flux ( $q''$ ) and mercury pressure in the vapor quality region of the plug insert shows a discontinuity at the end of the plug. This discontinuity is caused by the change in the internal geometry of the mercury flow passage. A similar discontinuity in the plot of the heat flux takes place at the end point of the tube quality section ( $X = 100\%$ ) because a different heat-transfer correlation is used in the superheat region. The mercury temperature assumed in the vapor quality region is the saturation temperature corresponding to the local calculated pressure.

#### PERFORMANCE HISTORY

The double-containment Ta-SS boiler was tested for 1445 hours at the NASA-Lewis Research Center. The primary objective was to obtain as much operating time as possible on the boiler in order to evaluate its endurance capability. In order to minimize the possibility of accidental shutdowns, system operating conditions were maintained relatively constant throughout testing. As a result, no performance maps were generated.

Four boiler parameters representative of its operating history are plotted in Fig. 10. Within the first 50 hours of operation, the mercury flow rate was increased to rated conditions. Due to a decrease in available power to the primary loop, it was necessary to lower the mercury flow rate after some 300 hours of operation. With

this one exception, the mercury flow was maintained constant throughout most of the testing. The three remaining parameters in Fig. 10 are indicative of overall boiler performance. The terminal temperature difference (average value 14° F), based on the NaK inlet temperature and an immersed thermocouple in the vapor stream at the boiler exit, indicates excellent performance throughout the run. The high degree of superheat and good vapor quality, present at the boiler exit throughout testing, (again based on vapor stream conditions) exemplifies the boiler's performance from a systems standpoint. Each of the four shutdowns listed in Fig. 10 were traceable to test-support equipment and in no way related to boiler performance. It should be noted that following each of these shutdowns, boiler exit conditions returned to preshutdown values. Throughout testing (including startups) the boiler exit pressure remain relatively steady and at no time did it oscillate by more than  $\pm 4$  psi.

#### COMPARISON WITH PREDICTED RESULTS

A significant result of boiler testing is the fact that the heat fluxes, as indicated by the NaK temperature profile in the open-tube boiler vaporization section, were higher than expected; in this respect, the boiler exceeded the design predictions. A comparison of analytical and experimental temperature and pressure profiles along the boiler length is shown in Fig. 11. In plotting the experimental pressure profile, it was necessary to estimate the mercury-side pressure at the plug-insert end based on the boiler overall pressure drop and a calculation of quality at the end of the plug section. An examination of the pressure plots shown in Fig. 11 reveals good agreement beyond the end of the plug insert. In the plug section the deviation in the pressure curves is traceable to a poor heat-transfer rate.

The experimental NaK temperature profile downstream of the plug insert indicates better-than-predicted heat transfer rates. In the plug insert section however, the profile indicates a poor heat transfer rate based on the slope of the experimental NaK temperature curve. It should be noted that in plotting this curve considerably more significance was attributed to the data of profile "A" based on a post-test examination of the boiler. The data scatter and relatively poor heat transfer rate indicated in the plug section can be explained by the fact that a significant coating of NaK oxide was found on the primary-NaK-flow surface of the oval stagnant-NaK-containment tube which evidently increased the thermal resistance in that area of the boiler. This inspection also disclosed a structural weakness in the tube bundle spacer-supports that caused the bundle to shift from its concentric location in the NaK shell. These conditions shifted the NaK flow and distorted the NaK-temperature profile as indicated by the shell thermocouples at locations "A" and "B" in Fig. 11.

The dropwise dry-wall boiling heat-transfer correlations (provided in Refs. 7 and 8) are based on the droplet vaporization model in the vortex two-phase flow regime.

For this reason, the design NaK profile refers to ideal heat transfer under nonwetting conditions. Possible wetting of the tantalum surface by mercury can be visualized as a cause for better boiling heat transfer in the region beyond approximately 6 feet.

A comparison of boiler parameters for the operating point shown in Fig. 11 is provided in Table 1. In compiling the data for Table I, the independent variables used in calculating the predicted results were chosen to match those of the test data wherever possible.

A comparison of the boiling heat flux distribution, in terms of quality, is shown in Fig. 12. Both Q/A plots, experimental and analytical, are of similar configuration. The experimentally obtained Q/A values in the plug insert region are below the design prediction. In the boiling region downstream of the plug insert ( $x = 0.10$  to  $0.75$ ), the experimental Q/A values were greater than the design predictions. This condition suggests that the tantalum surface was wetted by mercury. In the high-quality region above  $x$  of about  $0.7$ , the test data show decreasing Q/A values indicative of film boiling.

#### CONCLUDING REMARKS

Successful operation of the double-containment Ta-SS SNAP-8 boiler verified the soundness of the design and fabrication techniques used. Allowing for a change in the relative position of the tantalum tube within the flattened stainless steel tube proved to be a successful method for accommodating the large difference in tube expansion. The use of state-of-the-art welding techniques resulted in a structurally sound boiler, based on 1445 hours of operation. Boiler performance, including the effect of the NaK-filled double-containment design, was successfully predicted by analytical techniques. In fact, using tantalum as the mercury-containment material resulted in heat fluxes in the boiler vaporization section that were higher than expected. Finally, the degree of vapor superheat and the small terminal temperature difference which occurred immediately upon startup indicate the success with which the boiler fulfilled its design requirements.

#### REFERENCES

1. Anon., "AIAA Specialists Conference on Rankine Space Power Systems," AEC Rep. No. CONF-651026, Vol. 1, 1965.
2. J. A. Albers, W. T. Wintucky, and S. H. Gorland, "Conditioning and Steady-State Performance of SNAP-8 Tube-In-Shell Mercury Boiler," NASA TM X-1441, 1967.
3. A. H. Kreeger, J. N. Hodgson, and A. J. Sellers, "Development of the SNAP-8 Boiler," AIAA Specialists Conference on Rankine Space Power Systems, AEC Rep. No. CONF-651026, Vol. 1, pp. 285-306, 1965.
4. A. A. Schoenberg, and D. R. Packe, "Analysis of Pressure-Drop Function in Rankine Space Power Boilers With Discussion of Flow Maldistribution Implications," NASA TN D-4498, 1968.
5. A. S. Sellers, "SNAP-8 Tube-In-Tube Design Analysis," Aerojet-General Corp., TM 4803; 65-2-223, February 1965.
6. A. C. Spagnuolo, "Evaluation of Tantalum-to-Stainless-Steel Transition Joints", Proposed NASA Technical Memorandum.
7. R. G. Gido and A. Koestel, "The SNAP-2 Power Conversion System Topical Report No. 17, Mercury Boiling Research," TRW Rep. No. ER-4833, AEC No. NAA-SR-6309, October 1962.
8. R. G. Gido, et. al, "The SNAP-2 Power Conversion System Topical Report No. 12, Boiler Development," TRW Rep. No. 4521, AEC No. NAA-SR-6304, July 1961.
9. A. J. Sellers, G. M. Thur, and M. K. Wong, "Recent Developments in Heat Transfer and Development of the Mercury Boiler for the SNAP-8 System," Proceedings of the Conference on Application of High Temperature Instrumentation to Liquid-Metal Experiments, Argonne National Lab., Rept. ANL-7100, NASA CR-76450, pp. 573-632, 1965.
10. O. E. Dwyer, "Eddy Transport in Liquid-Metal Heat Transfer," Brookhaven National Lab., Rept. BNL-6046, February 1962.
11. A. J. Sellers, "Forced Convection Mercury Boiling - Experimental Investigation Using a Helical Multi-passage Plug Insert in a Once-Through Boiler," Aerojet-General Corp., TM 4934:67-459, 1967.

TABLE I. - COMPARISON OF TEST RESULTS WITH  
ANALYTICAL PREDICTIONS

	Test results	Predicted results
Thermal power input, kW	475*	488
Mercury flow rate, lb/hr	10 669	10 669
Mercury inlet pressure, psia	326.1	371.9
Mercury exit pressure, psia	213.4	213.4
Mercury inlet temperature, °F	396	396
Mercury exit temperature, °F	1 307	1 307
Mercury inlet orifice pressure drop, psi	61.2*	61.2
Mercury preheat section pressure drop, psi	0.4*	0.3
Plug insert vapor section pressure drop, psi	12.6*	59.3
Open tube section pressure drop, psi	38.5*	37.7
Quality at the end of the plug insert, %	7*	34.5
Liquid carry-over, %	2.7	0.0
Exit vapor superheat, °F	277	277
External heat loss, kW	12	12
NaK to mercury temperature difference at liquid-vapor interface, °F	108.2*	79
NaK to mercury temperature difference at boiler exit, °F	12.4	15
NaK flow rate, lb/hr	46 588	46 922
NaK inlet temperature, °F	1 319	1 322
NaK exit temperature, °F	1 153	1 153
NaK side pressure drop, psi	2.3	1.2

\*Calculated values based on available data.

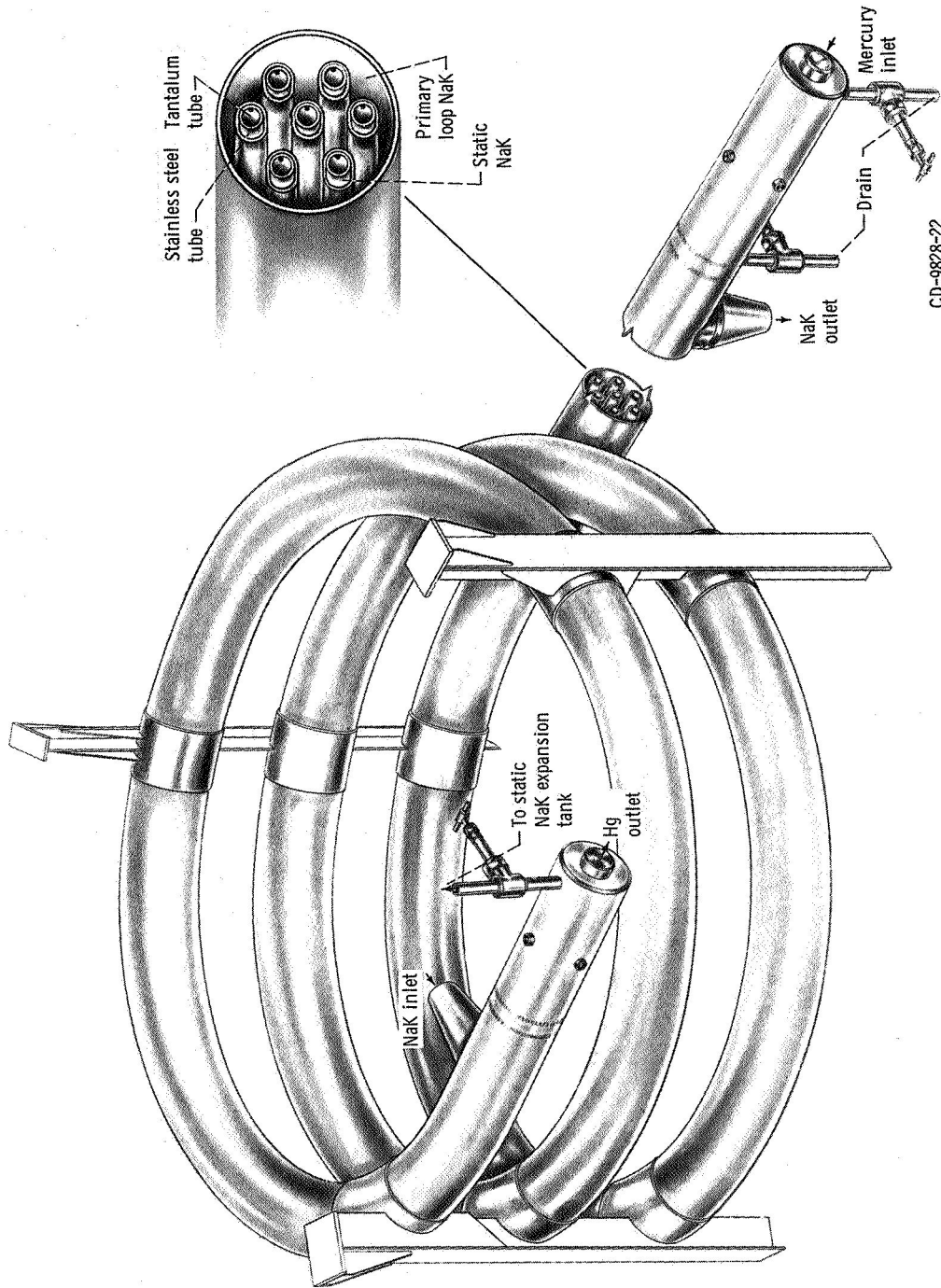


Figure 1(a). - SNAP-8 double containment Ta-SS boiler.

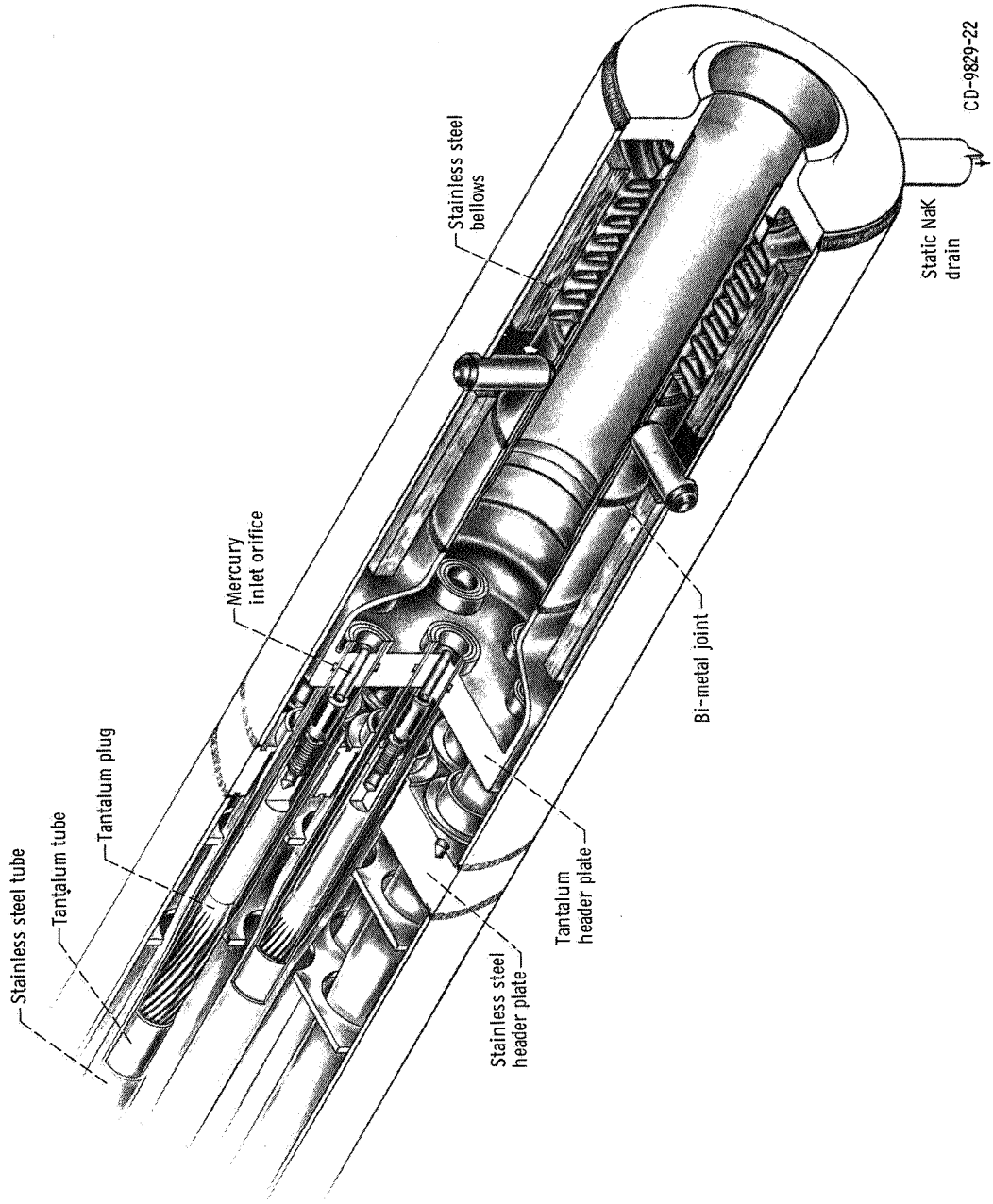
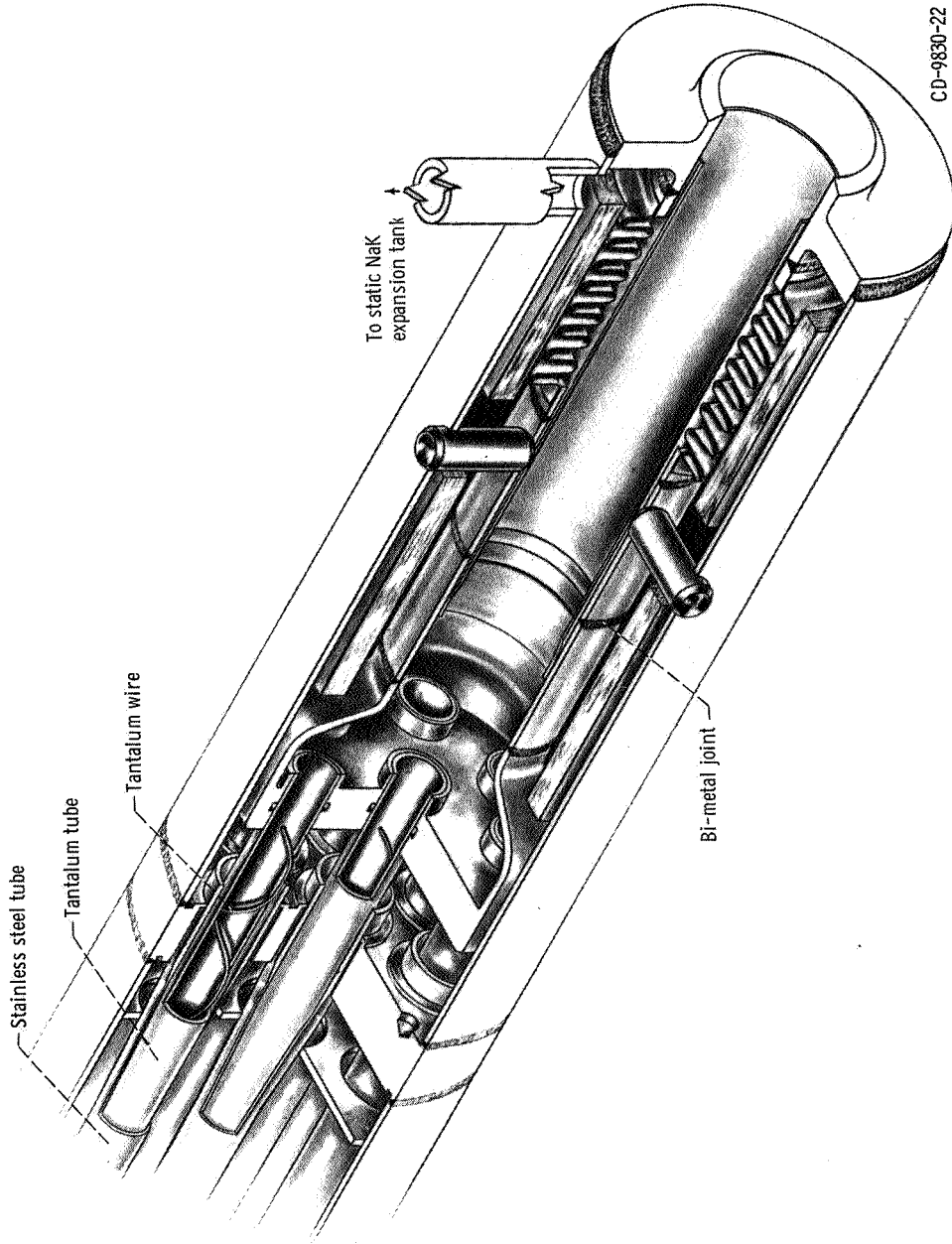


Figure 1(b). - Mercury inlet section.



CD-9830-22

Figure 1(c). - Mercury outlet section.

E-4501

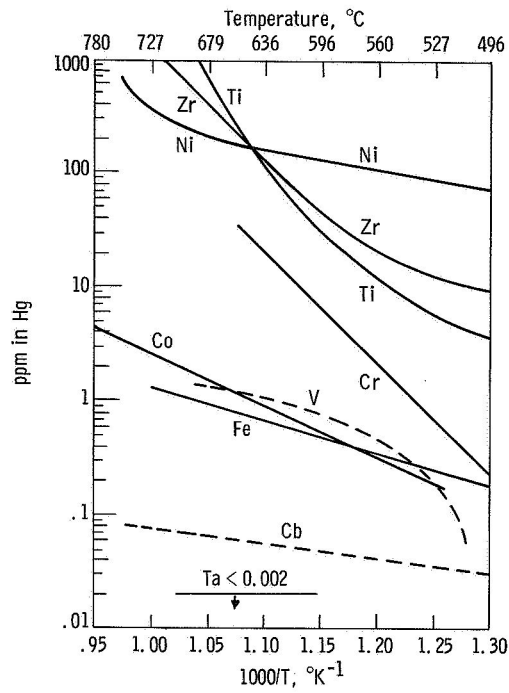


Figure 2. - Liquidus curves of metals in high temperature mercury.



Figure 3. - Tantalum within stainless steel tube bundle assembly.

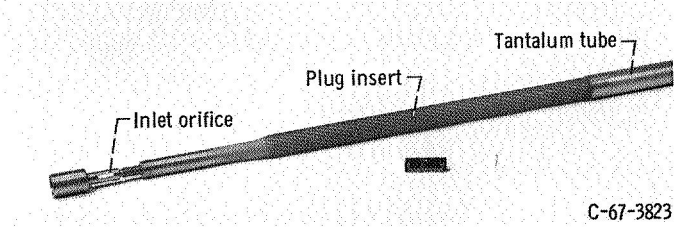


Figure 4. - Arrangement of inlet orifice, tantalum plug and tantalum tube.

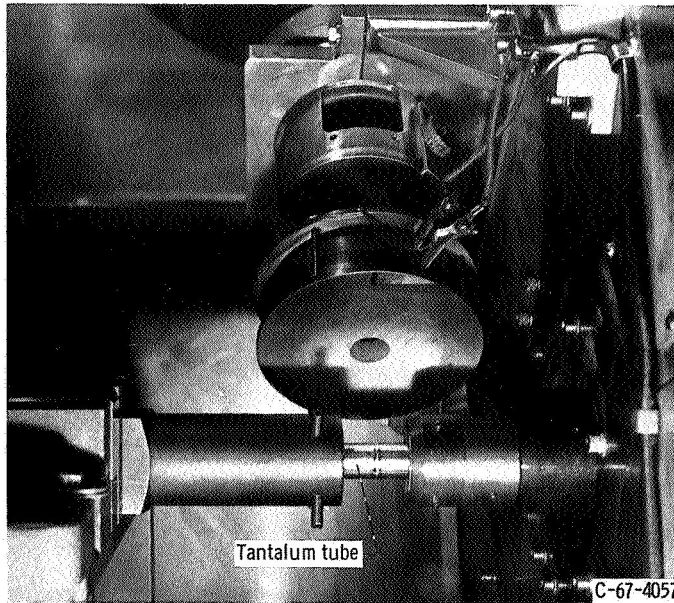


Figure 5. - Electron beam welding of tantalum tubing.

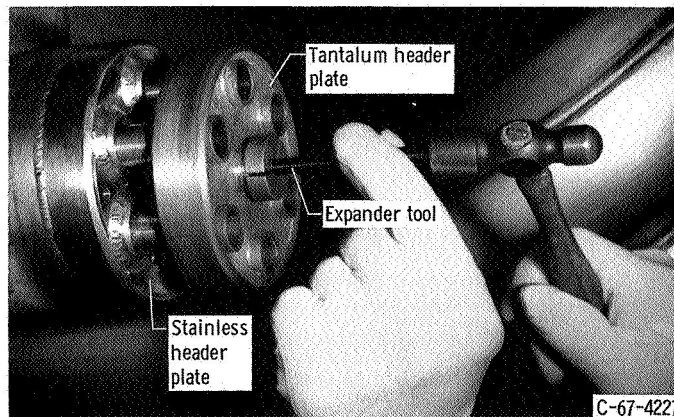


Figure 6. - Boiler header configuration.

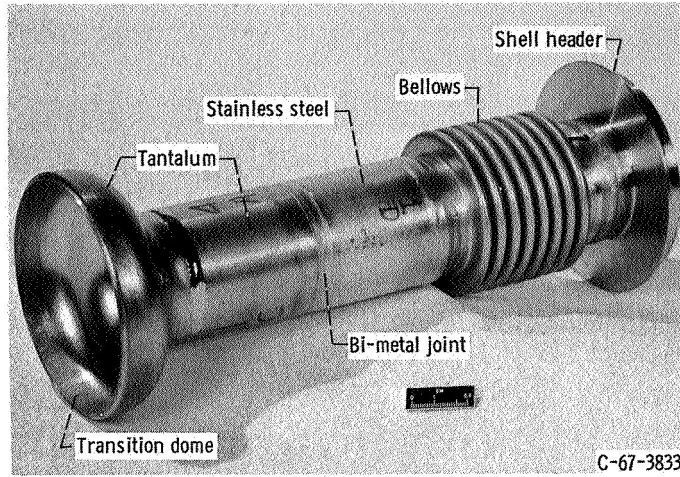


Figure 7. - Mercury inlet and outlet subassembly.

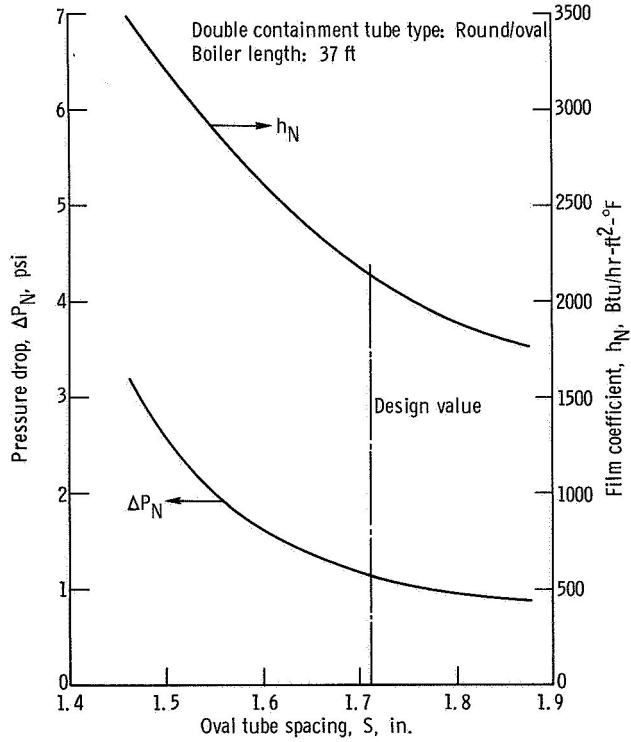


Figure 8. - Boiler NaK side pressure drop ( $\Delta P_N$ ) and film coefficient ( $h_N$ ) versus tube spacing (S).

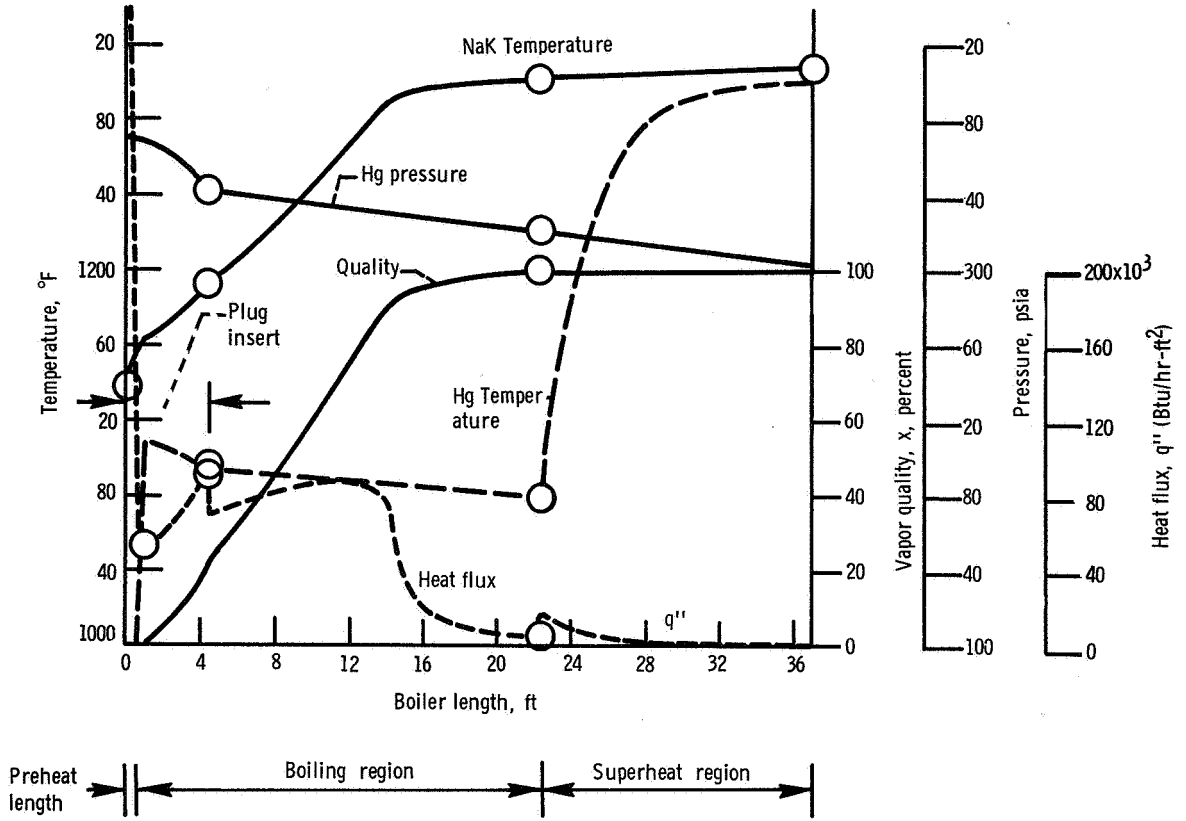


Figure 9. - Boiler performance characteristics (analytical).

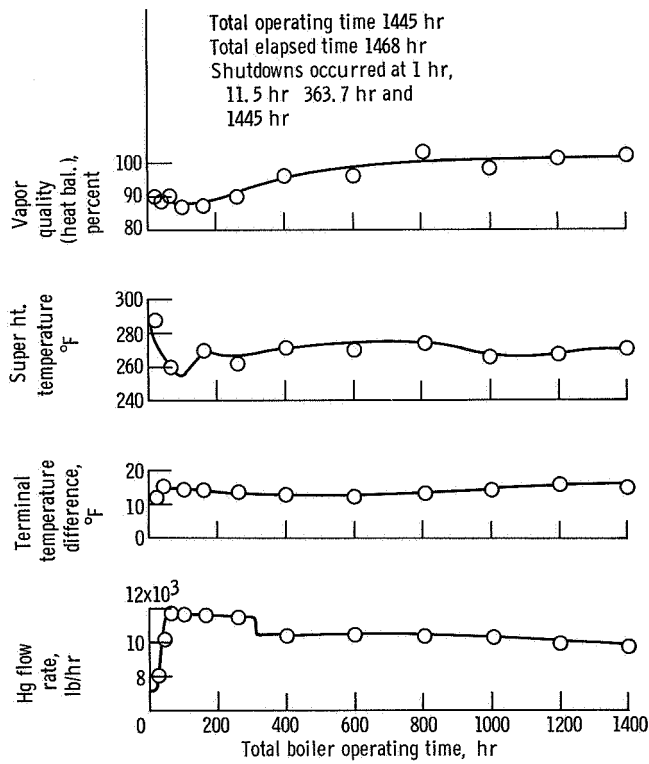


Figure 10. - Boiler operating history.

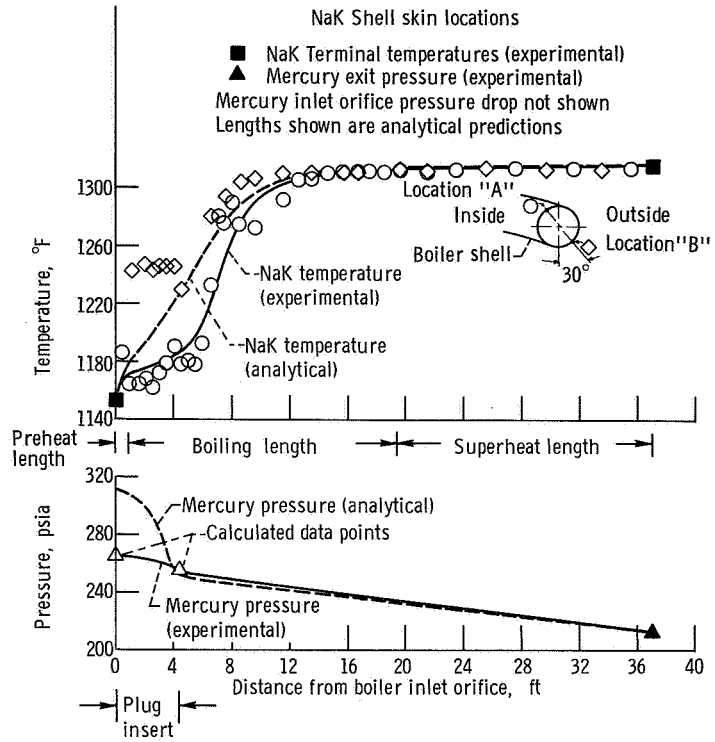


Figure 11. - Comparison of analytical and experimental temperature and pressure profiles.

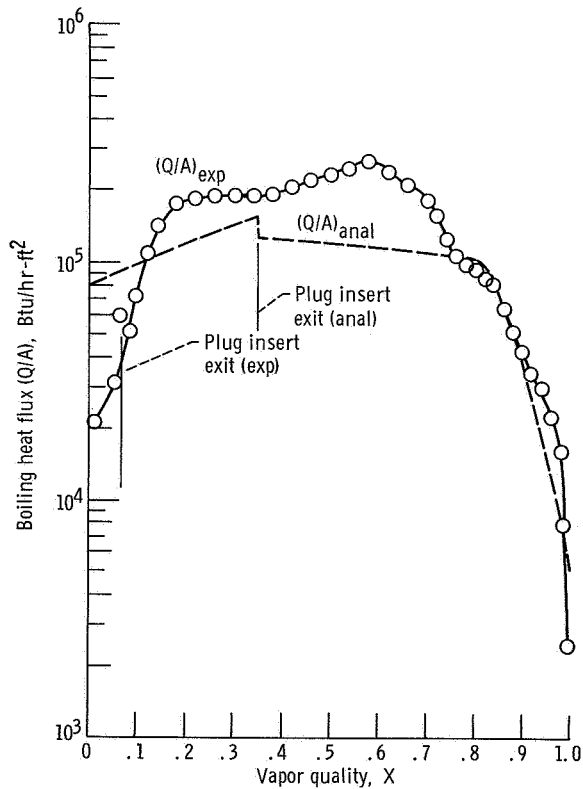


Figure 12. - Comparison of analytical and experimental boiler heat flux profiles.